

UC Irvine

UC Irvine Electronic Theses and Dissertations

Title

Creation of Soft Dome and Ball Actuators for Use with Vacuum Pressure

Permalink

<https://escholarship.org/uc/item/1fz090sb>

Author

Jitsiripol, Kevin Prameyoes

Publication Date

2020

Peer reviewed|Thesis/dissertation

UNIVERSITY OF CALIFORNIA,
IRVINE

Creation of Soft Dome and Ball Actuators for Use with Vacuum Pressure

THESIS

submitted in partial satisfaction of the requirements
for the degree of

MASTER OF SCIENCE

in Biomedical Engineering

by

Kevin Prameyoes Jitsiripol

Thesis Committee:
Associate Professor Elliot E. Hui, Chair
Professor Michelle Khine
Professor Abraham Lee

2020

DEDICATION

To my family and friends. For supporting me throughout this process
and putting a smile on my face.

TABLE OF CONTENTS

	Page
LIST OF FIGURES	iv.
LIST OF TABLES	v.
ACKNOWLEDGEMENTS	vi.
ABSTRACT	vii.
INTRODUCTION	1.
CHAPTER 1: BACKGROUND	2.
Pneumatic Control with Actuators	2.
Hui Lab Pneumatic Control Work	9.
Soft Pneumatic Actuators	12.
V-SPAs	13.
VAMPS	16.
CHAPTER 2: METHODS AND RESULTS	19.
Motivation for the Soft Actuator	19.
Fabrication of the Soft Actuator	20.
Test of Properties of the Soft Actuator	23.
Movement of the Lever Arm by the Actuator	27.
Load Testing of the Actuator	30.
Future Works with the Actuator	35.
CONCLUSION	36.
REFERENCES	37.

LIST OF FIGURES

		Page
Figure 1	Examples of Soft Robotics	1.
Figure 2	An Overview of the Octobot	3.
Figure 3	Schematic of a Soft Inverter	5.
Figure 4	Schematic of the Hexagonal Rolling Robot	6.
Figure 5	Schematic of the Size Separating Stage	7.
Figure 6	Overview of the Elastomeric Valves and Comparison between an NMOS inverter and an Elastomeric Actuator	10.
Figure 7	Overview of the Microfluidic Liquid Handling System	11.
Figure 8	Assembly of the V-SPA	13.
Figure 9	Two VAMPs Actuating Lifting a Load	17.
Figure 10	VAMP Moving a Skeletal Arm	18.
Figure 11	Image of the Mold for the Domes	20.
Figure 12	Image of the Dome Actuator	22.
Figure 13	Images of the Dome Actuators	23.
Figure 14	Measurement of the Speed of the Actuator	24.
Figure 15	Measurements of the Ball Actuator Size	26.
Figure 16	Lever Arm Movement by the Actuator	27.
Figure 17	Setup of the Sharpie Lever Arm	29.
Figure 18	Test for Return Force of the Actuator	31.
Figure 19	Contraction Force Test	32.
Figure 20	Lever Arm Moving 20 g	34.

LIST OF TABLES

		Page
Table 1	Volume Required to Actuate	23.
Table 2	Mass Measurements of the Coins	31.
Table 3	Comparison of the Performance of Actuators	35.

ACKNOWLEDGEMENTS

I would like to thank my committee chair, Associate Professor Elliot E. Hui. His research has inspired me to strive to achieve the best I can and explore the possibilities that are out in the world. He has given much direction to my research and helped when I was struggling or hit a roadblock. Without his help, this thesis would not have been possible.

I would like to thank my committee members, Professor Michelle Khine and Professor Abraham Lee, whose work has inspired me in the past and has helped me down the path I am on now.

In addition, I would like to thank all of my colleagues in Hui Lab for both being excellent colleagues and helping to sprout new ideas and solutions to issues that have come up in the course of my research.

ABSTRACT OF THE THESIS

Creation of Soft Dome and Ball Actuators for Use with Vacuum Pressure

by

Kevin Prameyoes Jitsiripol

Master of Science in Biomedical Engineering

University of California, Irvine, 2020

Associate Professor Elliot E. Hui, Chair

Soft robotics can provide alternatives from traditional robotics to grip, move, and assist in areas that are unsuitable to traditional robotics due to their hard shape and rigid structure. Pneumatic logic circuits developed in the Hui Lab hold strong potential for the control of soft robotics, but the technology can only drive vacuum actuators. In contrast, soft robotics are primarily designed to be driven by positive pressure. While a couple of notable vacuum actuators have been reported, they require the displacement of larger air volumes than can be generated by our lab's microfluidic circuitry. We set out to find a new actuator that is compatible with the previously made pneumatic logic controllers. The goal was to find a smaller actuator that could be used to run simple machines that was vacuum powered and had comparable properties to other actuators in the field. Soft ball and dome actuators were created from Dragon Skin 30 and either tygon tubing or a needle was used as an attachment to vacuum pressure. Through measuring displacement of a lever arm, recording the speed of the actuator, and measuring the load the actuator can move, the properties of the actuators were found and compared to those previously in the field. The actuators were shown to be able to provide mechanical advantage and be used in a simple machine by moving lever arms up and down by the change in vacuum pressure.

INTRODUCTION

Traditional robotics has a large impact on our current society, as many functions require the movement of hard, unyielding parts in order to work. However traditional robotics have inherent issues connected to them. They have a difficult time interfacing with humans due to the hard material and stiffness that they have and the rigidity of hard robotics leads to issues with movement through constrained spaces. Due to the fact that none of the parts used in traditional parts can deform, they cannot fit into smaller areas than what dimensions they have. Soft robotics can deal with these issues that occur with traditional robotics. Soft robotics is the use of traditional robotics techniques and creation of parts with soft materials that can deform. Soft materials are materials that are much more pliable such as Polydimethylsiloxane (PDMS) and other elastomers that can stretch and contract without any additional changes. Pneumatic soft robotics refers to using pressure differences in order to provide power to run these soft robotic structures. Soft robotics has been shown to have many good uses such as the creation of soft grippers, creation of a walking motion through a quadruped robot, and creating a glove to assist with grip strength by complementary movement with the hand as seen in figure 1 below. [1] [2] [3]



Figure 1: Example of Soft Robotics. A) A soft gripper actuated by pneumatics. [1] B) A glove that helps the user grip objects by adding additional force to the movement to the user. [2] C) A quadruped robot that is able to move by actuating specific parts [3]

Hui Lab has a strong emphasis on microfluidic logic and has used it as a pneumatic logic controller. These pneumatic logic controllers have strong potential to be used for soft robotics due to their speed and reliability in providing timing control for vacuum signals. However many of the current soft pneumatic actuators in the field are run through a positive pressure being supplied. This is a limitation due to the fact that our pneumatic logic controllers are run through a vacuum source and thus are incompatible with many of the different types of soft actuators that are currently being used for research. This was a strong motivator to find a soft pneumatic actuator that could be driven by vacuum that is compatible with the pneumatic logic controllers that the lab has. Throughout my research, I've created soft dome and ball actuators that are driven by vacuum. They are relatively simple to create and have the ability to be simply controlled with a single vacuum source powering them. These new actuators can be used in conjunction with vacuum microfluidic logic circuits in order to run complex oscillation patterns with multiple attached to a single circuit.

CHAPTER 1: BACKGROUND

Pneumatic Control with Actuators

There are previous examples of pneumatic control systems being used to run soft actuators. These include the octobot from the Wood group [4] and the entirely soft ring oscillator from Whitesides group. [5] The Wood group created an entirely soft robot that is controlled by microfluidic logic. It is made up of a soft microfluidic logic controller, fuel reservoirs, catalytic reaction chambers, actuator networks and vent orifices that are

surrounded by a soft octopus shaped body. [4] The catalytic reaction chamber has platinum that is incorporated into the soft elastomer in order to decompose the fuel to provide pressure to the majority of the octobot.

The control system of the octobot is separated into multiple parts as defined by the Woods group: upstream, oscillator, reaction chamber, and downstream. It begins at the upstream section, which contains the fuel storage. Figure 2 below shows the layout of the soft controller and the schematic view of the octobot and its process actuating.

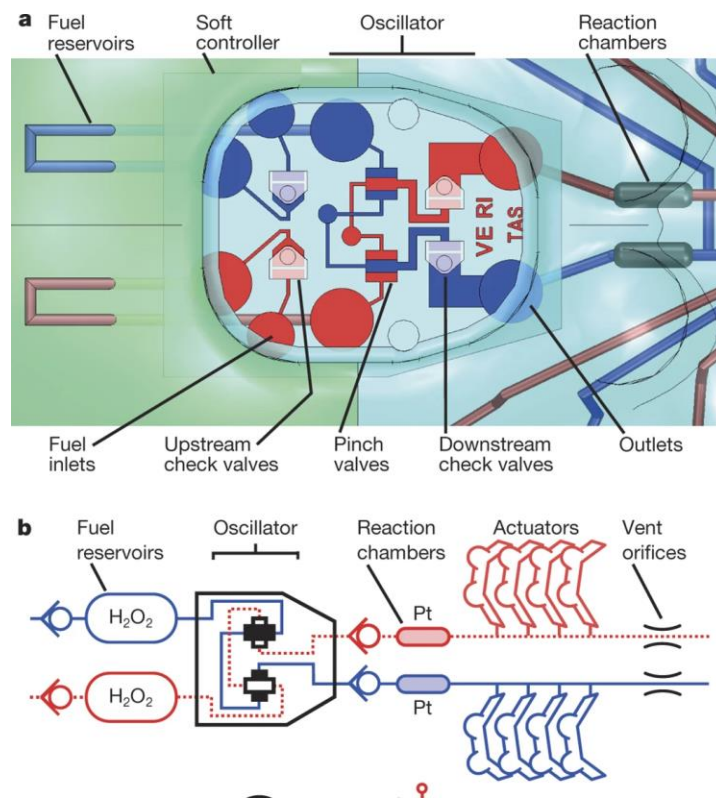


Figure 2: An Overview of the Octobot [4] A) Image showing the design of the soft controller. B) Layout of the octobot and the process to actuate the actuators.

The fuel that is used for this soft robot is hydrogen peroxide (H_2O_2) which is injected into two of the fuel reservoirs from two syringe pumps. Fuel flowing into these fuel reservoirs expands them elastically, which then forces fuel to enter the oscillator. The oscillator is made up of a series of pinch and check valves which convert the singular inlet flow into

an alternating fluid flow into two different outputs. Only one of the outputs flows outwards while the other is stopped. The flowing fuel then moves on to one of the two reaction chambers. In the presence of the platinum within the walls of the reaction chamber the hydrogen peroxide decomposes into water and oxygen through the reaction $2\text{H}_2\text{O}_2 (\text{l}) \rightarrow 2\text{H}_2\text{O} (\text{l,g}) + \text{O}_2 (\text{g})$. This pressurizes the gas down through one of the networks, which is made up of four actuators and a single orifice for venting. When the pressurized gas flows through the network, the actuators deflect and then the gas escapes the soft robot through the orifice. The deflection of the actuator leads to the lifting of the tentacles of the soft robot. After venting, the fuel flow stops in that network and begins in the other network, repeating the process in the other network. [4] The entirety of the process occurring within the robot leads to an alternating movement of the eight tentacles of the soft octobot.

Another important pneumatic control system is the soft ring oscillator is from the Whitesides group. [5] The soft ring oscillator is created from three different soft inverters being connected. The soft inverters are created from two different cylindrical chambers that are separated by a dome shaped membrane as seen in figure 3 on the next page. [5]

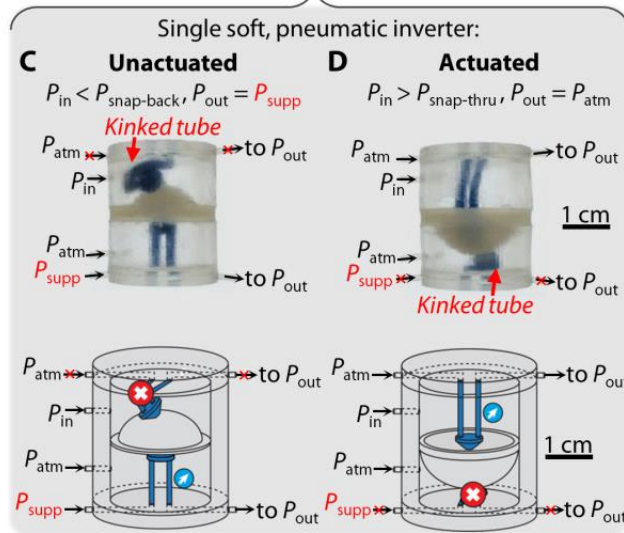


Figure 3: Schematic of a Soft Inverter. Shows the kinking of the tube constricting the pressure flow from the top or bottom chamber based on the direction of the central membrane.

Within the chambers, there is tubing connecting the two chambers through the hemispheric membrane. The bottom chamber of the inverter is connected to a variable input pressure while the top chamber is connected to atmospheric pressure. There is also a constant positive supply pressure that is supplied to the bottom chamber. Depending on the input pressure that is supplied to the top chamber the output pressure of the inverter changes. This is due to the kinking of tubing that occurs due to the deflection of the hemispheric membrane. The kinking of the tubing eliminates the flow of air in the upper or lower chambers. When the input pressure is low, the hemispheric membrane kinks the tubing within the top chamber, leading to the output pressure only being supplied by the bottom chamber and thus only the supply pressure. When the input pressure given is high enough, the membrane snaps through to the other chamber, leading to the bottom chamber's tubing to be kinked. This leads to the output pressure only being given by the atmospheric pressure instead. The atmospheric and supply pressure can be defined as two binary outputs of 0 and 1. This soft inverter

demonstrates the properties of an inverter by changing a low input pressure into the higher output supply pressure and changing a high input pressure into the lower atmospheric pressure.

Three of these are connected in order to create the soft ring oscillator. The three soft inverters are connected in series with one another. The output of one of the inverters becomes the input of the next inverter in series. [5] So if the output of one inverter is atmospheric pressure then the input into the next inverter would be atmospheric pressure. This leads to the three inverters constantly changing states between atmospheric pressure and supply pressure. This leads to a consistent oscillation occurring within the system as the state changes between the three different inverters.

The soft ring oscillator was shown to be used for multiple different uses in soft robotics. Some examples of this is their creation of a rolling soft robot and a size separating stage both being controlled by the soft ring oscillator.[5] In figure 4 below, the schematic of the soft rolling robot is shown below.

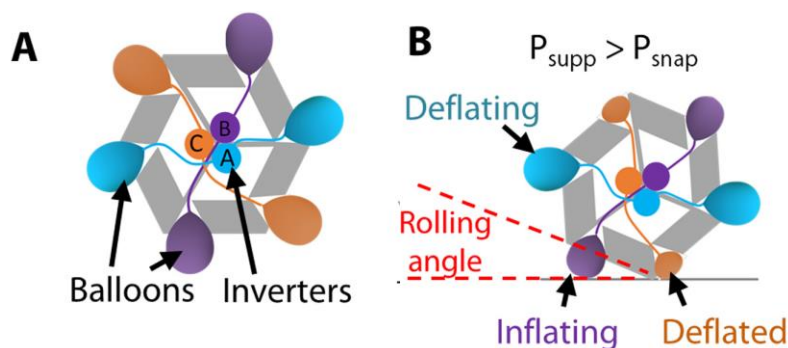


Figure 4: Schematic of the Hexagonal Rolling Robot [5] A) Schematic detailing the connections from the three inverters of the soft ring oscillator to the balloons actuators of the robot. B) Schematic showing how the robot inflates and deflates the actuators to create a rolling motion.

It has a hexagonal frame with six balloons. The balloons act as soft actuators for the hexagonal robot. The robot rolls from one face to another by the inflation and deflation of the balloons in sequence. The control of the robot is provided by the ring oscillator that is within the hexagonal frame. Each of the inverters provide pressure to two balloons on opposing faces. The balloons sequentially go through states of inflation, deflation, and completely deflated. The ring oscillator provides the timing to inflate the balloon on the bottom face of the robot. That balloon then begins deflating while the next balloon in sequence begins inflating in order to continue rolling the hexagonal robot along.

Another example of the use of the soft ring oscillator is the use in a size separating stage. [5] The size separating stage was created in order to separate particles of two different sizes. An image showing the layout of the size-separating stage is show in figure 5 below.

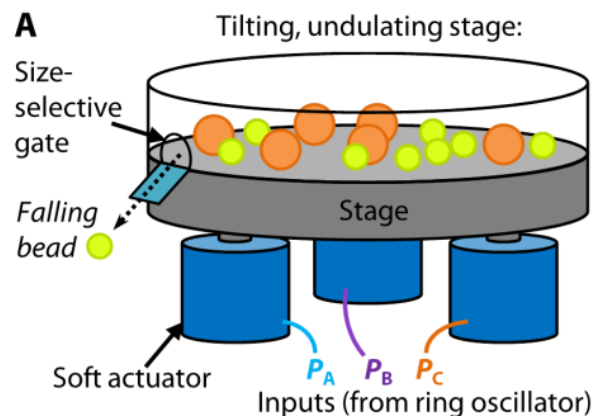


Figure 5: Schematic for the Size Separating Stage. [5]

The stage itself is created from a plastic disc that has an opening on the wall of the disc in between the size of the two particles. The stage is then mounted onto three linear soft actuators. These soft actuators are connected to the soft ring by the output pressure of

one of the three inverters. The individual outputs of each of the inverters becomes an input for one of the soft actuators. This translates the oscillation of the soft ring oscillator into the motion of the actuators. When the input pressure into the actuator is high, the actuator would extend upwards and while the input pressure into the actuator is low, the actuator would return to its original state. The size separating stage tilts based on how many actuators are extended or retracted. The nature of the soft ring oscillator switching inputs periodically translates to the circular movement of the stage. The circular movement of the stage leads to the circular movement of the particles within the stage. When the particles move around the stage only the smaller particles can escape due to the size of the gate being larger than the small particles but smaller than the large particles.

Both the octobot and the soft ring oscillator provide strong examples of the ability for pneumatic control to run soft robotics. Both rely on an oscillator created with no electronic components and instead are entirely run through changes in pressure within the controllers. Both have shown that these controllers can be connected with different kinds of soft actuators in order to convert the oscillating pressure of the oscillators into the mechanical movements of actuators. These methods have both strengths and weaknesses for the control of soft robotics.

Both of these systems have the benefit of being entirely soft systems. The lack of hard components allows for the integration of these systems to be integrated in robots that require an entirely soft system, such as a robot that is used within an organism. The system that is used by the Wood group requires a fuel source that is beyond a supplied air pressure, which increases the complexity of the system due to requiring an

additional fuel source to supply pressure to the octobot. The octobot requires a specific pressure source and cannot be run off of only a simple pressure source. Both system requires the use of positive pressure, which can lead to bursting of the components when over pressurized. Along with this neither of these systems would be compatible with the previous work from Hui Lab as the pneumatic controllers were made to be used with a vacuum source rather a positive source of pressure.

Hui Lab Pneumatic Control Work

There are previous works of pneumatic control work from the Hui Lab. One such example is in the paper, "Pneumatic oscillator circuits for timing and control of integrated microfluidics." [6] In many microfluidic systems, valves have to be actuated by a mechanical solenoid valves that have to be off-chip under computer control. This adds to the size and complexity of chips. The electronic components of circuits can be replicated with a pneumatic equivalent on chip instead. The basis of all of these pneumatic circuits is an equivalent of an electronic inverter. The resistor of an inverter is replaced by having a long length of serpentine, narrow channels as an equivalent. Having a long narrow channel will increase the resistance that will be experienced within the channels. Instead of power being given as a voltage differential, the pneumatic circuit is run by a pressure differential. The transistor is then replaced by an elastomeric valve instead. The microfluidic logic controller is made up of three layers, two glass layers and a PDMS membrane in the middle. Both layers of the glass have designs cut into it in order to create the areas for the channels and valves. The PDMS membrane in between the two had holes punctured in order to allow for the pressure from the power source to reach all parts of the inverter. For the inverter seen in figure 6,

[6] vacuum pressure is defined to be the supply and atmospheric pressure is defined to be ground. Analogous to NMOS logic, vacuum is defined to be a binary 1 while atmospheric pressure is defined to be a binary 0. The input of 1 opens the valve and gives an output of 0. An input of 0 leaves the valve closed and outputs 1 replicating the function of an electronic inverter.

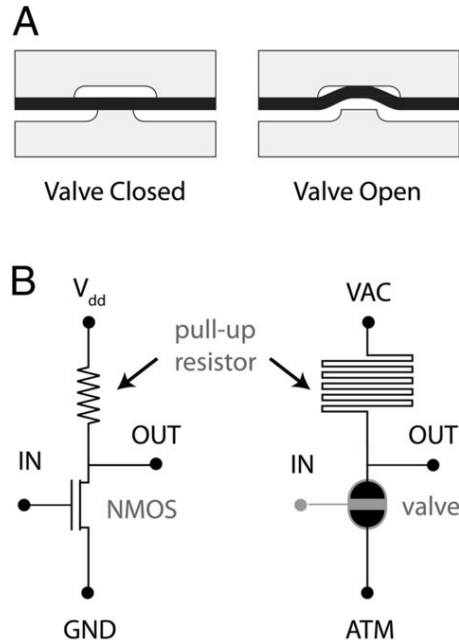


Figure 6: Overview of the Elastomeric Valves and Comparison between an NMOS inverter and an Elastomeric Actuator. [6] A) Shows the elastomeric valve within the microfluidic inverter. Valve opens with an input of 1 while the valve remains closed for input 0. B) Schematic showing the NMOS inverter and the analogous nature of the pneumatic vacuum inverter.

An important part for these vacuum-driven logic gates is that they have a high nonlinear gain. [6] Below a specific threshold pressure, the valve stays entirely closed. After a threshold pressure is passed, the valve fully opens quickly, which allows for binary outputs as there are two states that the inverter can inhabit without any states in between. An odd number of these inverters can be connected in a closed loop in order to create a ring oscillator. The output of one of the inverters becomes the input of the

next inverter within the loop. This leads to an alternating input of 0 and 1 to each of the inverters. This leads to a repeating oscillatory behavior in each of the inverters in the loop as each inverter flips between the two binary states.

Another example of the use of these vacuum microfluidic logic circuits is its usage in liquid handling. [7] The oscillator circuits that were previously mentioned can be used as a peristaltic pump in a liquid handling system. The valves of the three inverters open and close in sequence one after another, leading to a repeated opening and closing of the valves in the fluid handling portion one after another, proving a pumping force. The liquid handling system is made up of two oscillators, a combinatorial logic circuit, a pulldown network, and a fluid handling network. Based on the valves that are opened and closed, four different liquid handling processes will occur. They are metering, mixing, incubating, and washing. The combinatorial logic block is a series of valves and lines that are used in order to open and close specific groups of valves at the same time. Figure 7 below gives an overview of the actuator below. [7]

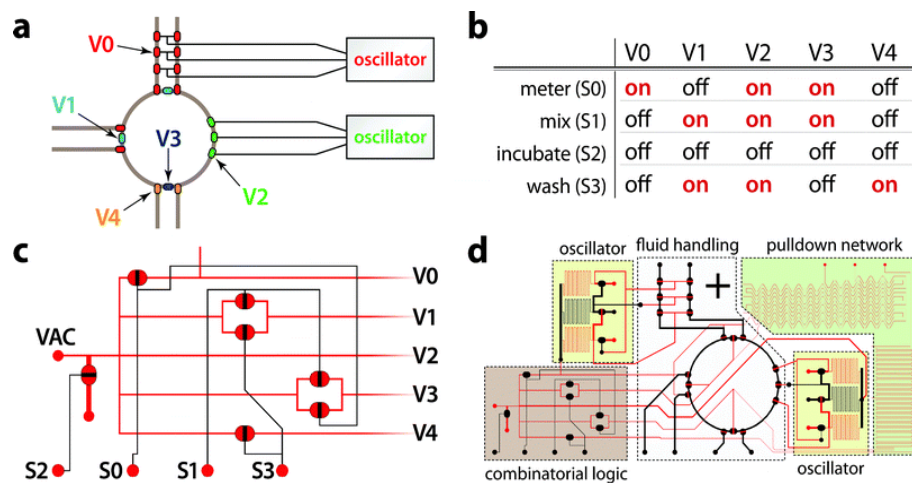


Figure 7: Overview of the Microfluidic Liquid Handling System [7] A) Overview of the grouping of valves that will open and close at the same time. B) Table showing the valves that are open and closed based on the process done by the circuit. C) Overview of the combinatorial block and the valves and lines that control each part of the circuit. D) Image showing the entirety of the circuit and all of its parts.

Each process needed for liquid handling has an input line in the combinatorial logic block that activates the specific valves that are needed for the liquid handling processes that are given. The liquid handling was shown by mixing blue and yellow food coloring using the device. Full mixing of the two food coloring was given by the color becoming uniform throughout. It was found that the device fully mixed the food coloring in fifty seconds. [7] Both of these processes have shown the usefulness of microfluidic logic in the timing and control of actions on chip. Components from the microfluidic can be used in order to control the flow of vacuum for soft robotics. This would allow for precise timing and control of the actuation of soft actuators.

Soft Pneumatic Actuators

Soft pneumatic actuators have been run both with positive and negative pressure. However there are issues that occur with positive pressure actuators. One of the main issues that occurs is that they can burst. When too much pressure is given to the actuator, the material structure of the actuator can fail and the actuator is destroyed. Along with that, they cannot decrease below their initial size when actuating, which makes them unsuitable for the use in any sort of space-constrained environment, such as moving within a tube with two different diameters. If the actuator only expands, the actuator must be smaller than the inner diameter in order to potentially function within the tube, limiting its design space. Vacuum-powered soft pneumatic actuators on the other hand, solve these issues. The usage of negative pressure avoids the issue of bursting, as actuators powered by negative pressure stop actuating when they reach a minimum size. As vacuum-powered soft actuators decrease in size when they actuate, they are more suited to move through constrained spaces with their decreasing volume.

There are two noteworthy previous examples of soft pneumatic actuators in V-SPAs and VAMPs. [8] [9]

V-SPA

An example of a soft vacuum actuator is from Jamie Paik's group with their work on what they refer to as a vacuum soft pneumatic actuator (V-SPA). [8] The actuator is created from two ovular pieces of foam separated by a hard paper divider surrounded by a skin of Elastosil M4601, a commercial elastomer. . The foam is 12.7 mm thick polyurethane. Paik's group used a CO₂ laser in order to cut out the foam shape, including the hollow core of the foam shape. [8] After that, the foam shapes and paper dividers are attached to a base plate by a mounting post. The foam pieces and paper dividers are assembled together by applying a cyanoacrylate gel between each of the layers. From there two coats of Elastosil M4601 were applied to the outside of the foam pieces and paper dividers using thin cardboard to brush on the elastomer to the foam. Figure showing the overview of the creation of the V-SPA is shown in figure 8 below.

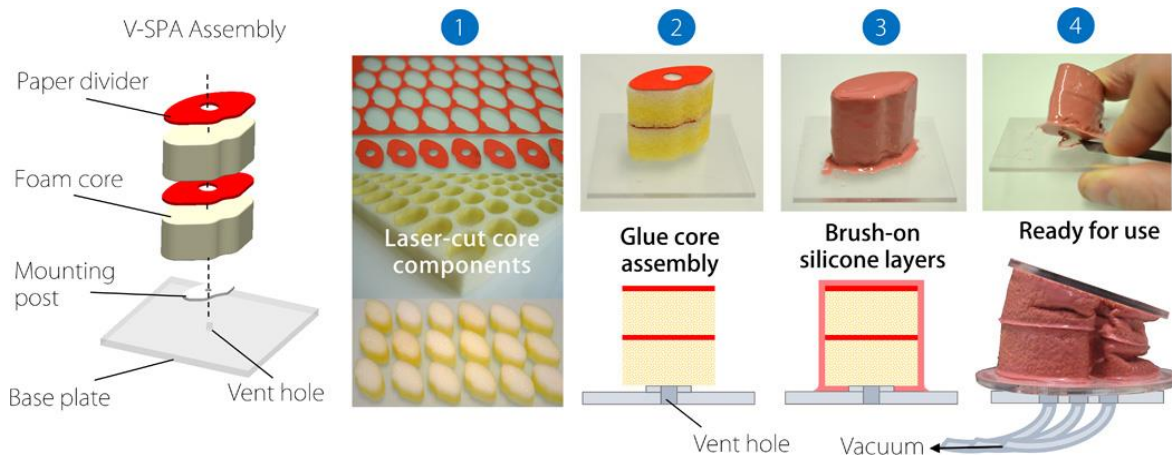


Figure 8: Assembly of the V-SPA [8]

There is a vent hole at the bottom of the base plate that attaches to a vacuum source through tubing attached to the base plate. Each of these make up a single V-SPA.

Three of these V-SPAs make up a singular V-SPA module. The three V-SPAs are assembled together in a circular shape. These are attached to two rigid base plates at the top and bottom. These plates house electronics, valves, pneumatic fittings, electrical connectors, and distribution channels to connect to a central vacuum supply in order to control the vacuum that is supplied to each of the individual V-SPAs. This allows for multiple V-SPA modules to be assembled together to perform various different functions.

An example of an application is multimodal locomotion using multiple V-SPA modules connected in series. They were assembled to provide two different gaits, a wave gait and a rolling gait. [8] The wave gait refers to the repeated pattern of actuations in sequence in order to move the entire structure forward. Forward in this case refers to the direction perpendicular to the flat face of the base plates and actuators. A rolling gait occurs due to actuating all of the actuators at once and sustaining the actuation of all of them. This leads to a lateral movement where structure rolls along the vertical walls of the actuators. The speed of the locomotion of the wave gait is 5 mm/s while the speed of the rolling gait is 60 mm/s. [8] The speed of the rolling gait is much faster than the speed of the wave gait, however this requires more open space as it moves perpendicular to the length of the multiple V-SPAs. This allows for the structure to move in multiple directions in 2-dimensions and be flexible in its applications. When there is more space to move, the rolling gait can be used in order to move quickly, while in more constrained spaces, the wave gait can be used to move through smaller areas.

Another is the application of the robot to climb windows/smooth surfaces. Multiple V-SPA modules are connected in series to one another with additional suction cups connected. From there, the actuator closest to the window/smooth surface actuates repeatedly in order to provide the motion for the actuator to climb up the surface, slowly crawling up a vertical surface. It was then shown to be able to move a mass of 70 g attached to the bottom of the robot in addition to the mass of the robot itself. [8]

The V-SPA and V-SPA modules have multiple positive and negative qualities. One of the major benefits of this actuator is that it was shown to be reconfigurable into many different forms based on the configuration of multiple V-SPA modules. It is not limited to any specific pattern for actuation and many locomotion modes such as vertical climbing, wave motions, and rolling motions can be done due to this flexibility in movement. However, this is only possible due to the creation of the full V-SPA modules, which require the incorporation of hard and electronic components. Another of the major strengths of the actuator is that the foam pieces act as a supporting structure for the actuator. This allows the wall structure for the actuator to be thinner than an entirely hollow structure. However, there is no comparison given for the wall thickness for these actuators compared to entirely hollow actuators. The individual measurements of the mass that the V-SPAs can lift was not given, however it was shown that V-SPA modules combined in series could lift up to 70 g as it was climbing up a smooth surface. For ideal fabrication of the device, it requires the use of a laser cutter to cut the foam pieces and paper dividers. This is a complicated piece of machinery needed to create the pieces for the actuator that is not available to everyone. In my own experience replicating the

design of the actuator, there were difficulties properly coating the outside of the foam pieces. As Elastosil M4601 was not easily available for purchase, I used an alternative in Dragon Skin 30, another commercial elastomer with similar properties to the Elastosil. However, the application of the liquid elastomer coating did not stick to the walls of the foam pieces and instead the elastomer would form a pool at the bottom of these actuators. This required the addition of a thickening agent for the elastomer to stick to the walls of the actuator. Along with that, if there are any leaks in the coat, the actuator will not function as the vacuum pressure will leak out of the actuator through any of the leakage holes. The size of an individual V-SPA has a width of 15 mm and a height of 45 mm. Along with that, the speed of the actuator contracting is 1.5 seconds and the returning to its original state is 2.7 seconds as stated from their testing as step rise and step decay time. [8] That is a relatively slow time for both the contraction and return of these V-SPAs. This hurts the ability for these V-SPAs to be used in time-sensitive situations as time will be lost to the time needed to contract and retract the actuators.

VAMP

Another important soft pneumatic actuator was created by the Whitesides group that they refer to as a vacuum-actuated muscle-inspired pneumatic structure (VAMP). [9] An important distinction is that the actuator was actuated by the buckling of elastomeric beams rather than a linear actuation. This resembles a muscle due to the built in structure and the fact that the actuator does not expand in the cross-sectional area when actuation occurs. The actuator is created from a 3D-printed mold that was designed within AutoCAD. This mold was made up of negatives of both vertical and horizontal pillars. This leads to a pattern of rectangles that when used as a mold would

lead to a series of horizontal and vertical pillars. The vertical pillars are larger than the horizontal pillars in order to direct the actuation vertically rather than actuating more in both vertical and horizontal directions. These molds are then filled with either Ecoflex 00-30 or Elastosil and then allowed to cure at room temperature. This creates a half of the actuator. These were then bonded together by applying uncured elastomers at the edges where they are bonded and then curing in an oven at 60 degrees for fifteen minutes. [9] The VAMP is connected to a vacuum source through tubing connecting from the top of the actuator. The effectiveness of the VAMP at providing a force was given by lifting two mass amounts with two VAMPs made out of different materials. The VAMP made out of Ecoflex was able to lift 20 g, while the VAMP made out of Elastosil was able to lift 500 g. [9] Although they had the same geometry, the VAMP created out of Elastosil was able to lift much more mass due to its higher Young's Modulus ($E = 520$ kPa) compared to the Ecoflex VAMP (43 kPa). Figure 9 below shows the structure of the VAMP when it actuates and the ability to lift a load mass. [9]

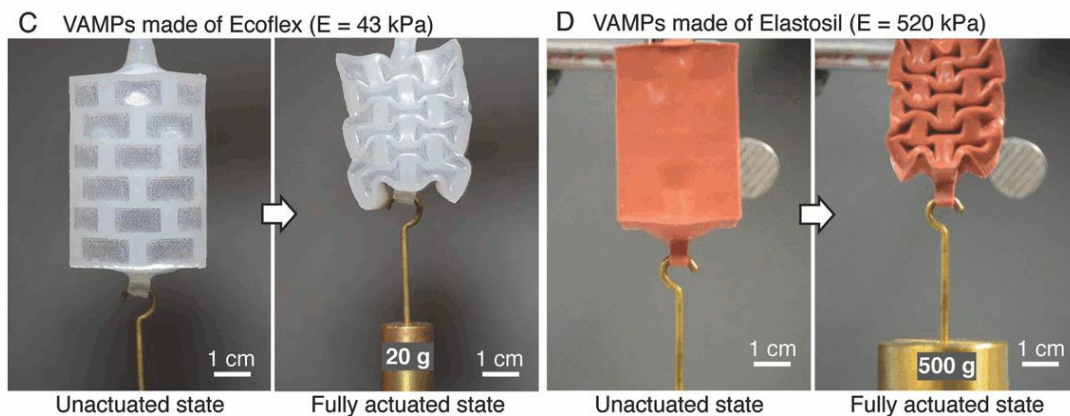


Figure 9: Two VAMPs Actuating Lifting a Load [9]

The VAMP was shown to be able to simulate muscle-like actuation through having a simulated skeleton arm move similarly to being moved by a bicep muscle

within the human body as seen in figure 10 below. [9] The actuator was found to have contracted 30% of its length and the displacement of the hand was found to have been 5 times the change in length of the VAMP. It is also shown to be able to lift a volleyball of mass 274 g. [3]

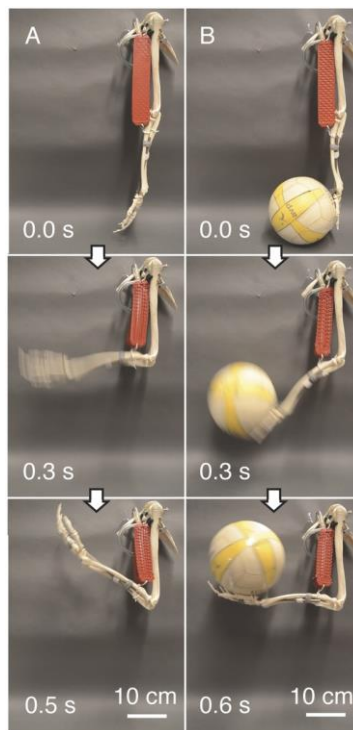


Figure 10: VAMP Moving a Skeletal Arm A) Moving with any mass. B) Moving a volleyball. [9]

One of the major benefits of the actuator is that it has the internal structure of pillars inside the actuator. This leads to the actuator having a movement that is fast and that is mainly linear in motion. The change in the vertical length of the actuator is large, as it is estimated to be around 40%. Meanwhile the change in horizontal width is much smaller as it is estimated to be around 5%. [9] Along with that, the VAMP was able to move a large amount of mass, as seen by the movement of the volleyball and the movement of both the 20g and 500 g weight. However, the use of the buckling pillars for the actuator increases the size that the actuator itself increases. Although an official

size of the actuators used in the tests was not given, we can use the scale bars given to estimate that the width of the actuator is at least 20 mm and the height of the actuator is at least 30 mm. That makes it a larger actuator that is non-ideal for the usage with microfluidic logic circuits as it would require a greater volume of air to be displaced in order to actuate when compared to a smaller actuator.

CHAPTER 2: METHODS AND RESULTS

Motivation for our Soft Vacuum Actuator

The previous soft vacuum actuators have been successes in their own right, however we wanted to create soft actuators that are in line with the use with our pneumatic control circuit. There is a need to have an actuator that is compact that can be comparable in load strength to the other actuators in the field. Both the V-SPA and the VAMP had concerns of being too large to be run with our vacuum microfluidic circuits, as they would both require a lot of air to be displaced in order to actuate both of them. The main design criteria of the actuator is having a fast operation time, enough force to move relevant masses, a long actuator stroke length, and to be made in a compact space. The design goals of the actuator are to have a time of operation faster than 5 seconds overall, enough force to move 15 grams, a stroke length at least 25% of the actuator length and require less than 12 cm³ of volume to actuate. We also needed to prove that the actuator could be used to translate its motion into a simple machine, such as a lever arm. During my time, testing the usage of other actuators with the microfluidic logic circuits of the lab, it was always a concern that the size of the other

actuators would not be actuated by the amount of air that would be displaced by the microfluidic logic circuits. A smaller actuator would be ideal as it would require less displacement of air in order to cause actuation compared to actuators of larger size.

Fabrication of the Soft Actuator

The soft actuators fabrication begins with an off-the-shelf mold from the company Miniature Sweet. It is a soft two-piece mold with both a cavity and a dome piece. The cavity has sizes of 14 mm, 12 mm, and 10 mm diameters. The dome piece is slightly smaller than the cavity piece in order to fit within. An image of the mold is given in figure 11 below.



Figure 11: Image of the Mold for the Domes

The actuator is created from a material called Dragon Skin 30. It is an elastomer that is made up of two individual parts with good strength at 592 kPa and flexibility at an elongation at break of 364%. These parts are mixed together in a one to one mass ratio and then degassed within a vacuum chamber for five minutes. Then the mixed Dragon Skin 30 is poured into the cavity and then the dome piece is then firmly pressed on top in order to prevent bubble formation and completely fill out the dome. The mold must then either cure for eighteen hours in room temperature air or be cured in the oven at 65 19.degrees for two hours. Hollow domes of three different sizes are made out of these molds. These actuators have various configurations that they are created in. They either

have a needle or syringe attachment and either are created in a dome shape, or a ball shape in any of the three diameters of 14 mm, 12 mm, or 10 mm.

The dome shaped actuator is fabricated by adding a bottom layer onto the dome. This is done by using a base plate of various materials, such as cardboard or polymethyl methacrylate (PMMA) to spread a layer of Dragon Skin 30. After the material is spread on, the hollow dome is pressed on top and then allowed to cure for the same time that the dome has. Pressure is gently applied to the base of the actuator in order to release the actuator from the base plate. The dome actuators were only made with a tygon tubing connector. The tubing was attached by pushing the tubing through a hole in the base plate into the dome itself. Afterwards, Dragon Skin 30 is spread around the hole in the base plate to create the bottom layer again. Along with that, Dragon Skin 30 is spread on the other side of the hole in order to secure the tubing in place. The bottom layer of the dome actuator is then cured and the layer is gently removed from the base plate. The layer supporting the tubing is also gently removed from the base plate. From there, the actuator can be connected to a syringe for use. The dome actuator can also be attached to the base plate without any negative impact on its function. The completion of both the actuator connected to tubing and the actuator connected to the base plate is shown in figure 12 on the next page.

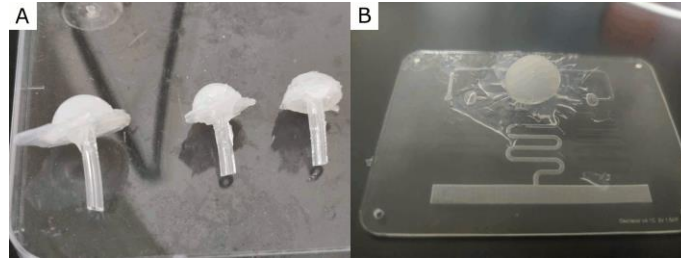


Figure 12: Image of the Dome Actuator: A) Connected to Tubing B) Attached to a Base Plate

The ball actuator is created from combining two of the hollow domes together. The two hollow domes are put into contact with each other at the circular edge of both of the hollow domes. The outside of the ball actuator has a layer of Dragon Skin 30 spread on around the area of contact between the two hollow domes in order to bond the two domes together. There is then a different method for the needle attachment or the tubing attachment to the ball actuator. For the needle attachment, the needle is used to puncture one of the round tops of the domes. From there another layer of Dragon Skin 30 is spread around the area that the needle punctures in order to secure the needle in place. From there it is allowed to cure for the allotted time given earlier. For the tubing attachment, a needle is again used to puncture the top of one of the hollow domes to create a hole to feed the tubing through. The tygon tubing is then fed through the hole and then Dragon Skin 30 is spread around the hole in order to secure the tubing to the ball structure. From there either of these are attached to needles in order to actuate the structure. Examples of the final ball actuators can be found in figure 13 on the next page.

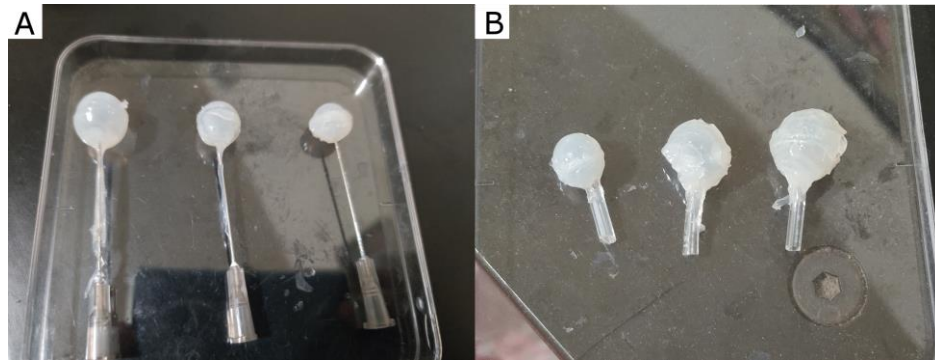


Figure 13: Images of the Ball Actuators A) With Needle Attachment B) With Tubing Attachment

Measurement of the Properties of the Actuators

The measurement of the volume of air displaced in order to actuate each of these actuators can be calculated from the measurement of the volume of the different actuators. The volume of the ball actuators can be calculated by the measurement of the volume of a sphere. The calculation for the volume of a sphere is $V = \frac{4}{3}\pi r^3$. For the dome actuators, the amount of volume within the actuator is measured by the volume of a sphere that is cut in half, which is $V = \frac{2}{3}\pi r^3$. As the diameter of the actuator is given by the molds themselves, a calculation of the maximum volume can be taken from that. The volume that needs to be displaced in order to provide actuation is given in table 1 below.

Table 1: Volume Required To Actuate Actuators		
Diameter of the Actuator	Dome or Ball	Volume Required to Actuate (cm ³)
10 mm	Dome	2.09
10 mm	Ball	4.18

12 mm	Dome	3.62
12 mm	Ball	7.24
14 mm	Dome	5.75
14 mm	Ball	11.5

From there, the speed of the actuator was measured for the actuator. The speed of the actuator was found by recording video of a 14 mm ball and dome actuator being entirely contracted by a syringe and then immediately being allowed to return back to its original size. The amount of time needed to contract the actuator can be defined as the contraction time and the time the actuator needs to return to its original state can be defined as its return time. To measure these two times, the video was measured frame by frame to find the time when the actuator is fully contracted and when it has returned to its original state. An example of the process is shown in figure 14 below.



Figure 14: Measurement of the Speed of the Actuator. A) Full contraction occurs at 0.85 seconds B) Return to the original state occurs at 2.15 seconds.

For the 14 mm ball actuator it was found that the contraction time occurred at 0.85 seconds. The time to return to its original state was found to be at 2.15 seconds. That would mean the return time was 1.3 seconds. The dome actuator was measured in the same method as the ball actuator above. It was found that the dome actuator had a contraction time of 0.43 seconds. It was then found that the actuator fully returned at the timestamp of 0.9 seconds. This means that the time for the actuator to return to its original state from a fully contracted state return time of the actuator was 0.47 s. It is consistent that both the contracting time and return time of the dome actuator was found to be faster than the contracting time and return time for the ball actuator. The displacement volume needed to actuate the dome actuator is half of the ball actuator, so it is expected that the contraction time and return time for the dome actuator to be faster than the contraction time and return time for the dome actuator. The speed of both the ball actuator and dome actuator was faster than the speed of the V-SPAs. The V-SPA had a contraction time of 1.5 seconds and a return time of 2.7 seconds. Both the ball actuator and dome actuator has an improved response speed compared to a previously built actuator. This allows it to be used in more time-sensitive usages with a higher efficacy as the actuator will spend less time going to a fully contracted state or return to its original state.

The percentage change in length of the actuators was found by measuring the change in width for the ball actuators and the measurement of the change in height for the dome actuators. The actuators used to measure the percentage change of the actuator were the two 14 mm actuators. The ball actuator was measured by placing it down onto a flat surface and aligning it with the zero of a ruler. The initial width of the

actuator was then measured. The images of the measurements are given in figure 15 below.

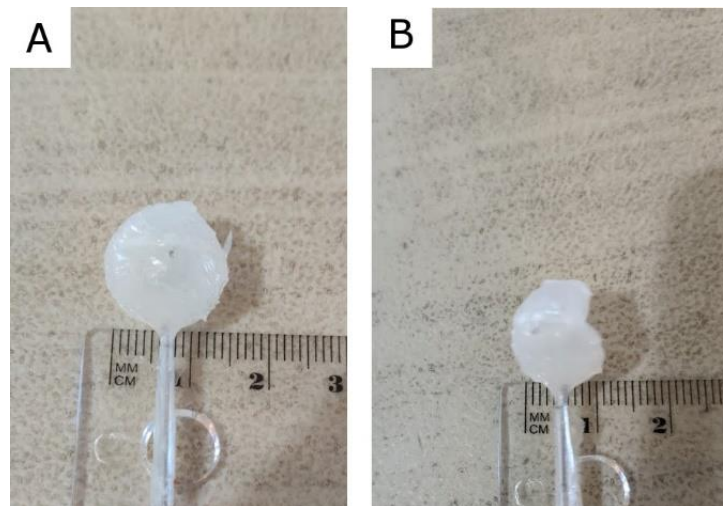


Figure 15: Measurements of the Ball Actuator Size at: A) Unactuated B) Fully Actuated

Then the actuator was then actuated by pulling air from a syringe and then measured from there. The actuator was found to have actuated from 14 mm to 9 mm. The change in actuator size was found to be 5 mm. Then the change of the actuator was divided by the size of the actuator in order to measure the percentage change of the actuator. This length change of the actuator was found to be 36%. This is similar to the actuation length of the VAMP. The movement of the actuator is comparable to other another actuator in the field despite its small size and the lack of structure within the actuator.

The change in length of the dome actuator was found similarly. The dome actuator was aligned with the ruler and then the initial height and final height of the actuator was measured from there. It was found that the initial height of the dome actuator is 7 mm and that the final height of the dome actuator is 5 mm. The percentage change of the actuator length is 28%. It is important to note that one of the major limitations for the change of length of the dome actuator is the tubing within the

actuator. The actuator cannot contract past the tubing of the actuator and will stop at the height of the actuator. There is potential that if the tubing of the actuator was mounted not as high within the interior of the actuator then the actuator could contract more than 28%.

Movement of a Lever Arm with the Actuator

The actuator was shown to provide movement by moving multiple lever arms by the movement of the actuators. The ball actuator was used in order to move the lever arms. The platform for the lever arm was a tissue box that had strings attached on by tape to the top of the tissue box. From there the lever arm has strings attached to one of its ends by attaching the other end of the string to the lever arm by tape. That anchors the lever arm to the base while allowing the rest of the lever arm to move freely. From there the ball actuator is put underneath near the lever arm's attachment to the string and attached to a syringe through the tubing of the actuator. This puts the pivot point near one of the ends of the lever arm. The lever arm is then moved up and down by the actuation of the actuator. Movement of the actuator is shown in figure 16 below.

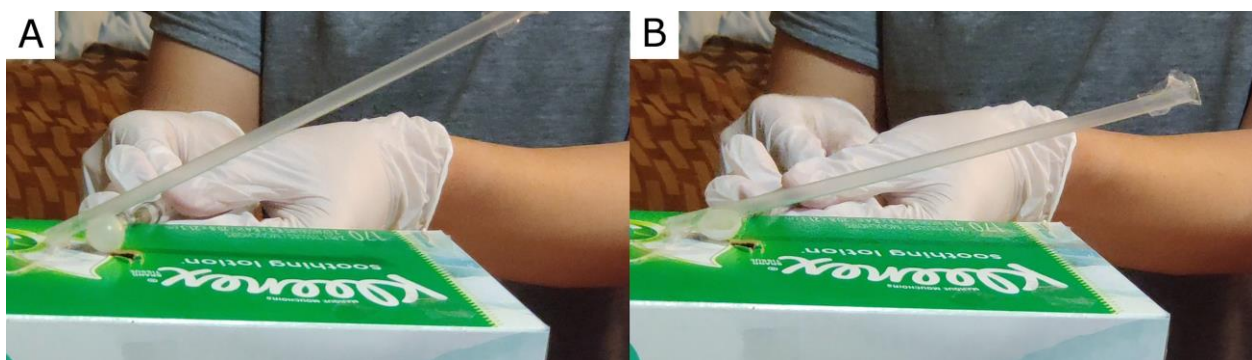


Figure 16: Lever Arm Movement by the Actuator: A) Unactuated B) Fully Actuated

The actuator is moved up and down by pulling air in and out of the actuator by pulling the plunger of the syringe back and forth. The actuator moved in a consistent manner

every time vacuum was applied as the same area of the actuator would collapse. That translated to the lever arm lowering the same amount every time as long as the distance of the actuator along the lever arm was consistent.

There are two lever arms that are moved by the actuator. These were a plastic straw and a sharpie. The straw was used in order to prove that the actuator could provide mechanical advantage and as a proof of concept that a lever arm could be moved. The initial and final heights of the lever arm was found by measuring the end of the lever arm at the time the actuator is unactuated and at the time the actuator is fully actuated. This is then compared to the measurements of the change in the ball actuator as given earlier. The initial height of the lever arm was at 12.7 cm. After actuation from the actuator the lever arm was moved to a height of 7.8 cm. This leads to a change of height of 4.6 cm. As given earlier, the ball actuator changed from 14 mm in width to 9 mm in width. A ratio of distance actuated in the ball actuator and the distance moved by the lever arm is calculated as a ratio of 1:9. This is greater than the measurement of the ratio given by the Whitesides group of the change in length of the VAMP and the displacement of the hand. The movement of this lever arm proves that the actuator can provide mechanical advantage through simple machinery by translating the movement of the actuator into another part such as a lever arm.

The angle of movement is found in order to show that the actuator actuates lever arms consistently despite changes in mass of the lever arm. This was confirmed by comparing the movement of a straw as a lever arm vs a sharpie as a lever arm. The sharpie was turned into a lever arm in a similar way to the straw lever arm. The sharpie was attached to the top of the tissue box through taping one end of the string onto the

end of the sharpie while another end is taped onto the top of the tissue box. The ball actuator was once again placed underneath the lever arm near the location where the lever arm is attached to the top of the tissue box by string. An image showing the setup of the sharpie lever arm is shown in figure 17 below.



Figure 17: Setup of the Sharpie Lever Arm

After the lever arm is properly set up, it was found that the lever arm started at 8.7 cm. After the lever arm was actuated by the ball actuator, it was found that the lever arm was then lowered to 4.8 cm. That is calculated to a change of 3.9 cm. The length of the lever arm is needed in order to compute the angle that the lever arm moved due to the actuator. The length of the sharpie was then measured to be 14 cm long. With the measurement of the length of the sharpie and the change in height from the force of actuation, the angle can be calculated from the inverse cosine of the height change in the lever arm over the length of the lever arm using the formula $A = \cos^{-1}\left(\frac{\text{opposite}}{\text{hypotenuse}}\right)$. From that calculation, it was found that the sharpie lever arm's angle of change was 15 degrees. The same calculation was made for the straw lever arm. The straw was

measured as 20 cm long. The change in height of the lever arm and the length of the lever arm was then used in order to find that the change in angle for the lever arm. That was found to be 13 degrees. The change in angle from one lever arm to another was shown to be similar to one another. This shows that there is a consistency in the actuation of the ball actuator usage to actuate a lever arm. Despite the sharpie being many times heavier than the straw, the angle that the lever arm moves through is the same.

Load Testing of the Actuator

The mass that the actuator can move both with the lever arm and by itself was then measured. Calculations for how much mass the actuator can directly move is desired due to the fact that this shows the forces that the actuator itself can produce. Two different forces were measured for the actuator, which are the restoring force or the contracting force. The restoring force refers to the force when the actuator returns from full actuation to its original shape. The contracting force is the force that is initially given by the actuator's force when it is actuating to full contraction. The restoring force and the contracting force was found through multiple tests.

The test for finding the restoring force was set up by creating a set of weights that was created from a set of standard US coins. The mass of the coins are available on the official US mint website and was confirmed by measuring their mass on a scale. [10]. A table showing the mass of the coins used is shown in Table 2.

Table 2: Mass Measurements of the Coins	
Coin Used	Mass of the Coin (g)
Dime	2.268
Nickel	5.000

When a larger mass than an individual coin was needed, the mass was made by attaching multiple coins to each other by adhering tape to surround the coins used. In order to measure the force of the actuator rebounding, the actuator was first pulled into its full contraction state. The mass that is being measured was then placed on top of the actuator and the pressure is allowed to return to the actuator. An example of the experimental setup is shown in figure 18 below.



Figure 18: Test for Return Force of the Actuator

If the actuator was able to return to its original state, it was able to apply a force greater than that amount. The maximum amount of mass that the actuator moved due to its restoring force was a mass of five nickels. This is a mass amount of 25 g that was able

to be moved by the actuator. When the mass amount is increased to five nickels and one dime, the actuator is unable to return to its original state which means the mass that the actuator cannot lift is 27.268 g.

The test to find the contracting force was done by attaching one of the coins directly to the actuator by applying Dragon Skin 30 to both the face of the coin and the area of attachment to the actuator in order to be able to connect the coins to the face of the actuator. From there the attachment between the actuator and the coin was allowed to cure for the standard time at room temperature. From there any additional weight was attached by applying a single layer of tape on the face of two different coins. This allows for the coins to adhere better to more pieces of tape due to providing a better surface for the tape to adhere to. From there a single piece of tape is rolled in order to create a double sided piece of tape. This piece is then placed in between the two coins' faces with tape in order to adhere the coins together. This process is repeated until the actuator could not lift the mass of coins that was being used. The actuator is then actuated with the coins hanging downward in order to see if the mass has moved when the actuator has a vacuum applied. An example of the test is shown in the figure below

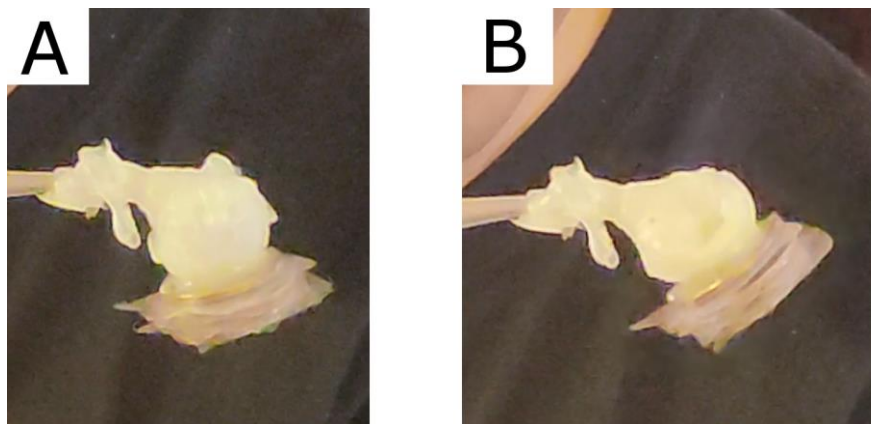


Figure 19: Contraction Force Test. A) Actuator is Unactuated B) Actuator Contracts Moving the Mass of Coins Upward

It was found that the actuator was able to move a coin amount of eight dimes. This is equal to a mass of 18.144 g being pulled by the actuator. The amount that the actuator can move is greater for its returning force than its contracting force. That means that the actuator is limited by the amount that can be pulled in any process that requires upward movement of the actuator.

Compared to the force that both the V-SPA modules and VAMP could produce, the ball actuator did not produce as much contracting force as either of the two. However, it is uncertain how much force an individual V-SPA could produce as their measurements of force were with two entire modules lifting a maximum of 70 g. There is a possibility that the ball actuator could lift a similar load to an individual V-SPA, but there is not enough data to conclude that. The ball actuator is not as strong as some of the other actuators in the field, likely due to the unstructured nature of the inside of the actuator and it is one of the weaknesses of the ball/dome actuator.

From there, the actuator was measured to see how much could be lifted at the end of a lever arm. The sharpie lever arm was used due to the fact that it could handle more weight at the end of the lever arm without deformation. The straw would bend due to its mass compared to the mass of coins at the end of the actuator. In order to add the coin mass to the end of the actuator arm the coin mass was attached to a length of string by attaching it to a face of one of the coins by tape. The string is then attached to the end of the lever arm by adhering tape to the end of the lever arm. Multiple coins are combined to create a single mass in a similar way to the contracting force test by applying a layer of tape on both sides, and then applying a layer of tape wrapped around to have the adhesive layer on both sides of the coins with a flat layer of tape. In

order to measure the maximum mass that the actuator can move, various mass amounts were attached to the end of the lever arm and then the actuator was actuated through a syringe pulling air from the actuator. If the actuator is able to return and return the lever arm to its original position, it was considered that the actuator was able to apply enough force to move the mass given. If the actuator was unable to move the lever arm, it was considered that it was beyond the load that the actuator can move. From the measurements of the mass actuated, it was found that the maximum mass that the actuator could actuate was 20 g at maximum. Beyond that with four nickels and a penny, a mass of 22.5 g, it was found that the lever arm would collapse, but not return to its original state. The actuation is shown in figure 20 below. Note that the lever arm movement is smaller due to the placement of the actuator nearer the center of the sharpie rather than the base of the lever arm. It goes from above parallel to parallel.

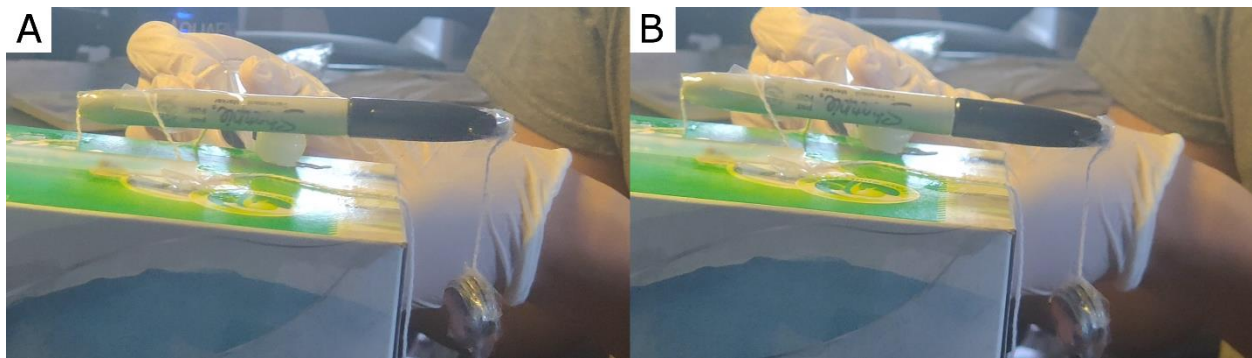


Figure 20: Lever Arm Moving 20 g. A) From Unactuated B) To Actuated

The actuation of the lever arm has shown to be able to be done with an increased weight at the end of the lever arm. For example, this allows for the lever arm to carry a load along with the lever arm itself such as moving a small robotic arm that holds a small ball bearing in its hand. The increased weight at the end of the lever arm and the subsequent change in center of mass does not prevent the actuator from moving the

lever arm and load. This shows the flexibility of the actuator when it is being used with a lever arm and that it can do more than only move a lever arm alone. Table 3 on the next page compares the performance of the ball actuator to the performance of the V-SPA and the VAMP.

Table 3: Comparison of the Performance of Actuators			
Characteristic Measured	Ball and Dome Actuator	V-SPA	VAMP
Volume Displaced Required to Actuate (cm ³)	2.09-11.5	Data Not Reported	Data Not Reported
Contraction Time (seconds)	0.85 (Ball) 0.43 (Dome)	1.5	Data Not Reported
Return Time (seconds)	1.3 (Ball) 0.47 (Dome)	2.7	Data Not Reported
Percentage Change in Length	36% (Ball) 28% (Dome)	Data Not Reported	30%
Ratio of Change in Length of Actuator and Lever Arm Displacement	1:9	Data Not Reported	1:5
Angle Displaced by the Actuator	13-15°	Data Not Reported	Data Not Reported
Restoring Force (g)	25	Data Not Reported	Data Not Reported
Contracting Force (g)	18	70 (V-SPA Module)	20 (Ecoflex) 500 (Elastosil)

Future Works with the Actuator

This is a new type of actuator that is easy to fabricate, has comparable strength properties to other actuators and can be assembled from simply a liquid elastomer and off the shelf components. This potentially gives it uses in limited resource countries as it has simple fabrication methods and simple materials. The small size of these actuators makes them ideal for their usage with the vacuum microfluidic digital logic that our lab uses. The volume of air displaced in order to move the actuator is closer to the amount

of air that the microfluidic digital logic can move rather than the larger actuators of the V-SPA and VAMP. Their small size also allows for their use in smaller scale robots as well which would want a size-appropriate actuator to be used. The actuator can also potentially be used in order to run more dexterous tasks such as being the joints to move fingers in a hand.

CONCLUSION

This is the first step in creating an actuator that is well-suited for use with vacuum microfluidic logic. The use of vacuum to actuate these actuators makes them compatible with the vacuum-run microfluidics of Hui Lab. It is an actuator that has properties comparable to the others but within a smaller size. That size allows the actuator to require less volume of air to be removed to fully actuate the actuator better matching the amount of air that the microfluidic logic circuits can remove. It also allows for its usage when more compact tasks are needed to be done. The efficacy of the actuator was measured through the speed, the actuation length of the actuator, the restoring force, and the contracting force. The actuators usage in soft robotics was proven with a simple machine in moving a lever arm and a lever arm with an additional weight at the end. The future goal of this actuator would be to prove its usage with more complicated machines and implement it fully within a vacuum microfluidic logic control system.

References

- [1] Ilievski, F., Mazzeo, A. D., Shepherd, R. F., Chen, X., & Whitesides, G. M. (2011). Soft Robotics for Chemists. *Angewandte Chemie International Edition*, 50(8), 1890–1895. <https://doi.org/10.1002/anie.201006464>
- [2] Whitesides, G. M. (2018). Soft Robotics. *Angewandte Chemie International Edition*, 57(16), 4258–4273. <https://doi.org/10.1002/anie.201800907>
- [3] Tolley, M. T., Shepherd, R. F., Mosadegh, B., Galloway, K. C., Wehner, M., Karpelson, M., Wood, R. J., & Whitesides, G. M. (2014). A Resilient, Untethered Soft Robot. *Soft Robotics*, 1(3), 213–223. <https://doi.org/10.1089/soro.2014.0008>
- [4] Wehner, M., Truby, R. L., Fitzgerald, D. J., Mosadegh, B., Whitesides, G. M., Lewis, J. A., & Wood, R. J. (2016). An integrated design and fabrication strategy for entirely soft, autonomous robots. *Nature*, 536(7617), 451–455. <https://doi.org/10.1038/nature19100>
- [5] Preston, D. J., Jiang, H. J., Sanchez, V., Rothmund, P., Rawson, J., Nemitz, M. P., Lee, W. K., Suo, Z., Walsh, C. J., & Whitesides, G. M. (2019). A soft ring oscillator. *Science Robotics*, 4(31). <https://doi.org/10.1126/scirobotics.aaw5496>
- [6] Duncan, P. N., Nguyen, T. V., & Hui, E. E. (2013). Pneumatic oscillator circuits for timing and control of integrated microfluidics. *Proceedings of the National Academy of Sciences of the United States of America*, 110(45), 18104–18109. <https://doi.org/10.1073/pnas.1310254110>
- [7] Nguyen, T. V., Duncan, P. N., Ahrar, S., & Hui, E. E. (2012). Semi-autonomous liquid handling via on-chip pneumatic digital logic. *Lab on a Chip*, 12(20), 3991–3994. <https://doi.org/10.1039/c2lc40466d>
- [8] Robertson, M. A., & Paik, J. (2017). New soft robots really suck: Vacuum-powered systems empower diverse capabilities. *Science Robotics*, 2(9). <https://doi.org/10.1126/scirobotics.aan6357>
- [9] Yang, D., Verma, M. S., So, J.-H., Mosadegh, B., Keplinger, C., Lee, B., Khashai, F., Lossner, E., Suo, Z., & Whitesides, G. M. (2016). Buckling Pneumatic Linear Actuators Inspired by Muscle. *Advanced Materials Technologies*, 1(3), 1600055. <https://doi.org/10.1002/admt.201600055>
- [10] *Coin Specifications | U.S. Mint*. (n.d.). Retrieved May 24, 2020, from <https://www.usmint.gov/learn/coin-and-medal-programs/coin-specifications>